Simulating Dynamic Loads on Concrete Components using the MM-ALE (Eulerian) Solver

Jiing Koon Poon[1], Shih Kwang Tay[1], Roger Chan[1], and Len Schwer[2]

[1]Ministry of Home Affairs, Singapore
[2]Schwer Engineering & Consulting Services

Abstract

Concrete components can either be modeled as Lagrangian or MM-ALE solids. This paper provides an overview of various concrete material models available in LS-DYNA® for use with the MM-ALE solver under the simple load case of unconfined compression. The manuscript concludes with a case study of the behavior of concrete panels subjected to air blast.

1 Introduction

Identifying suitable concrete material models to be used in conjunction with the Multi-Material Arbitrary Eulerian Lagrange[1] (MM-ALE) solver is of interest to Ministry of Home Affairs (MHA) Singapore, as part of a long-term technology development programme to study close-in, contact and near contact blast effects on structural elements [1, 2]. When simulating close-in and contact blast scenarios, there are two key drawbacks when using a coupled Eulerian-Lagrangian approach, with the air and detonation products modeled using Eulerian elements and the concrete components modeled using Lagrange elements. The first is the “leakage” issue due to the penalty based Fluid-Structure Interaction interface between the expanding detonation gases and the concrete components due to the large differences in the densities of the two components. The second is the element distortion issue, requiring possible element deletion via an ad hoc erosion criterion.

The alternate to Lagrange element formulation for solids is MM-ALE. To check the accuracy of the existing concrete material models using MM-ALE, previous work was performed by MHA comparing the results of two simple quasi-static conditions of uniaxial strain and uniaxial stress using *MAT_005 (Soil_And_Foam) and *MAT_072R3 (Concrete_Damage_Rel 3) [3]. It was reported that damage in *MAT_072R3 was accumulated unrealistically rapidly when a slight movement of material was detected. The implication is that if the concrete component is expected to deform significantly during an event, e.g. close-in or contact blast, the resultant residual strength, e.g. residual axial capacity, obtained from the model may be much lower than reality.

This paper presents an overview of the various concrete material models available in LS-DYNA for the use with MM-ALE under the simple load case of unconfined compression (quasi-static condition), and study the behaviour of a concrete panel subjected to air blast (dynamic condition), by comparing the simulated results with experimental data.

2 Concrete Material Models

LS-DYNA has several concrete material models which have the ability to auto-generate the necessary full suite of input parameters, including an Equation-Of-State (EOS), by specifying a minimum number of parameters, e.g. the unconfined compressive strength. These models include *MAT_016 (Pseudo_Tensor), *MAT_072R3, *MAT_085 (Winfrith_Concrete), *MAT_159 (CSCM), *MAT_272 (RHT) and *MAT_273 (Concrete_Damage_Plastic_Model). Of these models, only *MAT_016 is indicated as available with MM-ALE.

[1] In LS-DYNA terminology, MM-ALE is used even when referring to the Eulerian solver used in this manuscript.

*MAT_016 is assigned Category 8B for use with the MM-ALE which comes with a disclaimer stating that “error associated with advection inherently leads to state variables that may be inconsistent with nonlinear constitutive routines and thus may lead to nonphysical results, non-conservation of energy, and even numerical instability in some cases”. Another material model that can be used when MM-ALE concrete is modeled is *MAT_010 (Elastic_ Plastic_Hydro) which is also labeled with the 8B caution.

*MAT_005 was assigned Category 8A which comes with a “validated” tag besides saying that it supports MM-ALE solid element formulation in LS-DYNA. The meaning of “validated” is not provided and in any case is misused in this context.

*MAT_005, *MAT_010, and *MAT_016 were chosen to be studied in this paper as the following can be defined in the models; i) pressure dependent yield surface, ii) pressure cutoff for tensile fracture, iii) bulk unloading modulus, and iv) Equation-Of-State. Though *MAT_005 and *MAT_010 do not have the ability to auto-generate its input parameters like *MAT_016, the input parameters in *MAT_005 and *MAT_010 can be calibrated from either experimental data for tri-axial stress tests, or from the results of tri-axial stress test simulations using concrete material models which are able to auto-generate input parameters, such as *MAT_016.

The unconfined compressive strength for the concrete to be used in this study is 32MPa. The calibrated *MAT_005 and *MAT_010 input, and *MAT_016 input invoking the auto-generation of all the input parameters by specifying the unconfined compressive strength, are shown in Figures 1 to 3.

```
*MAT_SOIL_AND_FOAM
$#     mid        ro         g      bulk        a0        a1        a2        pc
         1 2.1200E-3 11157.167 74381.228 26.268058 16.816316  1.189408    -1.010
$#     vcr       ref      lcid
     0.000     0.000         0
$#    eps1      eps2      eps3      eps4      eps5      eps6      eps7      eps8
     0.000 0.0573000  0.094800  0.111600  0.128700    0.1455    0.1626    0.1776
$#    eps9     eps10
    0.1890    0.2118
$#      p1        p2        p3        p4        p5        p6        p7        p8
     0.000       250       500      1000      1500      2000      2500      3000
$#      p9       p10
      3500      4500
```

*Fig.1: Calibrated *MAT_005 input for unconfined compressive strength of 32MPa*

To ensure that the material cards for *MAT_005, *MAT_010 and *MAT_016 are correctly specified with respect to the defined unconfined compressive strength of 32MPa, single element simulations using a Lagrangian solid element undergoing unconfined compression at a quasi-static strain rate of 0.01 per second, to check that the unconfined compressive strength of 32MPa is achieved in the simulations. The results from the 3 materials are plotted on the same graph in Figure 4.

As shown in Figure 4, *MAT_005, *MAT_010, and *MAT_016 all achieved maximum axial stress of 32MPa for the simulated unconfined compression, which corresponds to the specified 32MPa unconfined compressive strength.

```
*MAT_ELASTIC_PLASTIC_HYDRO_SPALL
$ Material Type 10 (units: Newtons-millimeter-millisecond-MPa)
$---+----1----+----2----+----3----+----4----+----5----+----6----+----7----+----8
$      MID        RO         G      SIG0        EH        PC        FS     CHARL
        10   2.30E-3   11.58E3      9.46       0.0      -1.0
$       A1        A2     SPALL
      2.24    -0.012       3.0
$     EPS1      EPS2      EPS3      EPS4      EPS5      EPS6      EPS7      EPS8

$     EPS9     EPS10     EPS11     EPS12     EPS13     EPS14     EPS15     EPS16

$      ES1       ES2       ES3       ES4       ES5       ES6       ES7       ES8

$      ES9      ES10      ES11      ES12      ES13      ES14      ES15      ES16

$
*EOS_TABULATED_COMPACTION
$---+----1----+----2----+----3----+----4----+----5----+----6----+----7----+----8
$    EOSID      GAMA        E0        V0
        10
$             EPS1                EPS2                EPS3                EPS4                EPS5
          0.00E+00             -1.5E-3             -4.3E-3           -1.01E-02             3.05E-2
$             EPS6                EPS7                EPS8                EPS9               EPS10
           5.13E-2             7.26E-2             9.43E-2             1.74E-1             2.08E-1
$               P1                  P2                  P3                  P4                  P5
              0.00               22.32               48,65               78.10              148.39
$               P6                  P7                  P8                  P9                 P10
            223.81              317.53              485.78             2836.16             4337.91
$               T1                  T2                  T3                  T4                  T5

$               T6                  T7                  T8                  T9                 T10

$             Kun1                Kun2                Kun3                Kun4                Kun5
            1.49E4              1.49E4            1.51E4                1.58E4              1.88E4
$             Kun6                Kun7                Kun8                Kun9               Kun10
            21.9E4              2.49E4              2.71E4              6.11E4            7.44E4
$ - - - - - - - - - - - - - - - - - - - - - - - - - - - - - - - - - - - - - - - -
```

*Fig.2: *MAT_010 input for unconfined compressive strength of 32MPa*

```
*MAT_PSEUDO_TENSOR
$#     mid        ro         g        pr
         3  2.120E-3         0     0.200
$#    sigf        a0        a1        a2       a0f       a1f        b1       per
    32.000      -145     0.000     0.000     0.000     0.000     0.000     0.000
$#      er       prr      sigy      etan       lcp       lcr
     0.000     0.000     0.000     0.000         0         0
$#      x1        x2        x3        x4        x5        x6        x7        x8
     0.000     0.000     0.000     0.000     0.000     0.000     0.000     0.000
$#      x9       x10       x11       x12       x13       x14       x15       x16
     0.000     0.000     0.000     0.000     0.000     0.000     0.000     0.000
$#     ys1       ys2       ys3       ys4       ys5       ys6       ys7       ys8
     0.000     0.000     0.000     0.000     0.000     0.000     0.000     0.000
$#     ys9      ys10      ys11      ys12      ys13      ys14      ys15      ys16
     0.000     0.000     0.000     0.000     0.000     0.000     0.000     0.000
```

*Fig.3: *MAT_016 input for unconfined compressive strength of 32MPa*

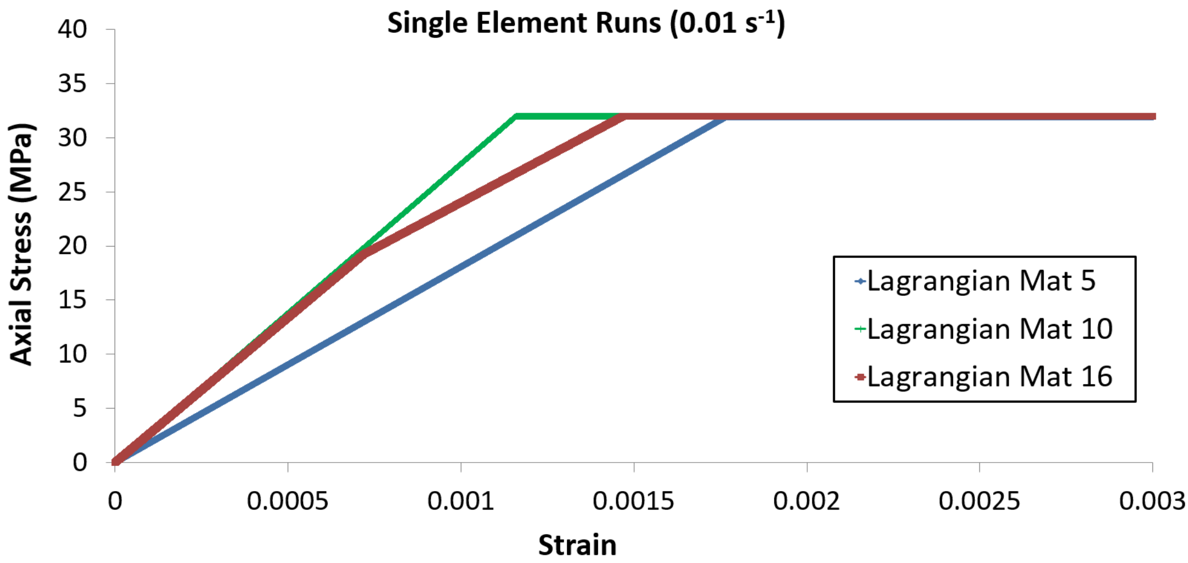

Fig.4: Single element runs at strain rate of 0.01 per second

3 Simulating Concrete Using MM-ALE

Multi-element MM-ALE models of a concrete column surrounded by air were created to investigate the response of different concrete material models under quasi-static unconfined compression.

The concrete column has a square cross-section measuring 300mm by 300mm, and a length of 1000mm. A 100mm-thick air layer was included to allow for lateral advection of the concrete material, which was expected due to Poisson effect when compressed in the axial direction. The same concrete material model inputs for *MAT_005, *MAT_010, and *MAT_016 as shown previously in Figures 1 to 3 were used. The nodes at one of the extreme Y-Z planes were fixed in the axial direction, while those at the other end were loaded in the axial direction by prescribed velocity to simulate compression loading. A screenshot of the models is shown in Figure 5.

For comparison, the same configuration was modeled with Lagrangian solid elements, with the same material model parameters. The only exception was that the air surrounding the column was not modeled since it was not necessary. The strain rate of 0.01 per second is considered for this study.

Figures 6 to 8 show the plots of the axial stress against strain for the Lagrangian and MM-ALE models across the three different material models used for the concrete column at the applied strain rate of 0.01 per second.

To obtain the axial stress of the column, the nodal forces of a set of nodes at the fixed end of the column is obtained using the keyword *DATABASE_NODAL_FORCE_GROUP. Aggregating these nodal forces will give the total axial load, and the axial stresses of the column can then be determined by dividing the axial load with the cross sectional area.

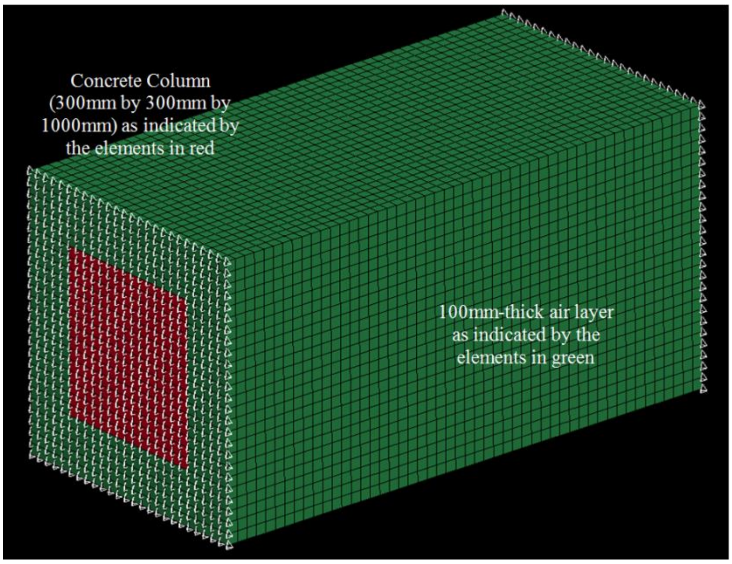

Fig.5: Screenshot of model showing 2 node sets at either end where one end is fixed in displacement in the axial direction, and the other is applying the axial load via velocity to the nodes

As shown in Figures 6 to 8, all the Lagrangian models achieved a maximum axial stress of 32MPa, equal to the unconfined compressive strength defined for the models. Assuming that the strain rate of 0.01 per second is quasi-static, the results verified that the Lagrangian models exhibited the correct compressive strength.

Upon reaching the maximum axial stress, *MAT_005 Lagrangian model registered a sudden unload of the axial stress to zero. This is due to the pressure experienced by the elements reaching the “pressure cutoff” value defined in the material card at the time when it unloaded, or failed. Refer to Figure 9 for a fringe plot of mean stress versus time for 3 randomly selected elements within the column, where it shows the “pressure cutoff” value of -1.01MPa is reached at around 178 msec where at the same time, the maximum axial stress is being obtained. This phenomenon will not be shown in the single element model of unconfined compression since there is no confining pressure and thus the mean stress will always be zero or positive. Shortly after unloading, the axial stress in the *MAT_005 Lagrangian model unexpectedly increased again with continuing axial velocity applied to one end of the concrete column. Since this is non-physical, the data presented after the unloading hence makes no sense and should be ignored.

*MAT_010 Lagrangian model registered a sudden unload of the axial load to zero upon reaching a maximum. This is due to the SPALL being set to 3 in the *MAT_010 input, where the material fails in tension, the stresses are set to zero and tensile mean stress is not allowed. Refer to Figure 10 for a fringe plot of mean stress versus time for 3 randomly selected elements within the column, where it shows the mean stress reaches zero at around 117 msec where at the same time, the maximum axial stress is being obtained. This phenomenon will not be shown in the single element model of unconfined compression since there is no confining pressure and thus the mean stress will always be zero or positive.

*MAT_016 Lagrangian model did not exhibit failure since there is no unloading in the plot. This is expected since no failure model other than “pressure cutoff” is defined in the *MAT_016 inputs. The “pressure cutoff” values for both *MAT_010 and *MAT_016 were checked and not achieved in the models.

As for the MM-ALE models, the *MAT_005 model gave a similar response to its Lagrangian counterpart. Near the point of peak axial stress, the response of the MM-ALE model deviated slightly from that of the Lagrangian model, achieving a slightly lower peak axial stress at a slightly later time. Similar to its Lagrangian counterpart, the *MAT_005 MM-ALE model registered a sudden unload upon reaching the maximum axial stress.

*MAT_010 MM-ALE model attained a slightly lower peak axial stress at about the same time when compared to its Lagrangian counterpart. *MAT_016 MM-ALE model produced a very different response than its Lagrangian counterpart. *MAT_016 MM-ALE model attained lower peak axial stress, and at an earlier time than its Lagrangian counterpart. There is no explanation for these observations.

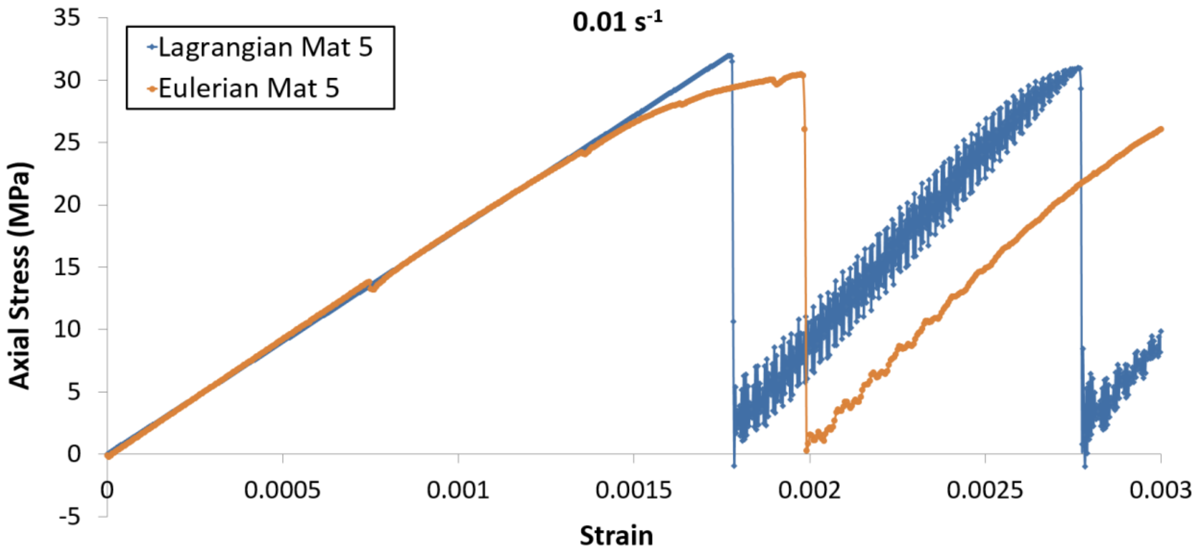

*Fig.6: Axial stress-strain curve at strain rate of 0.01 per second (*MAT_005)*

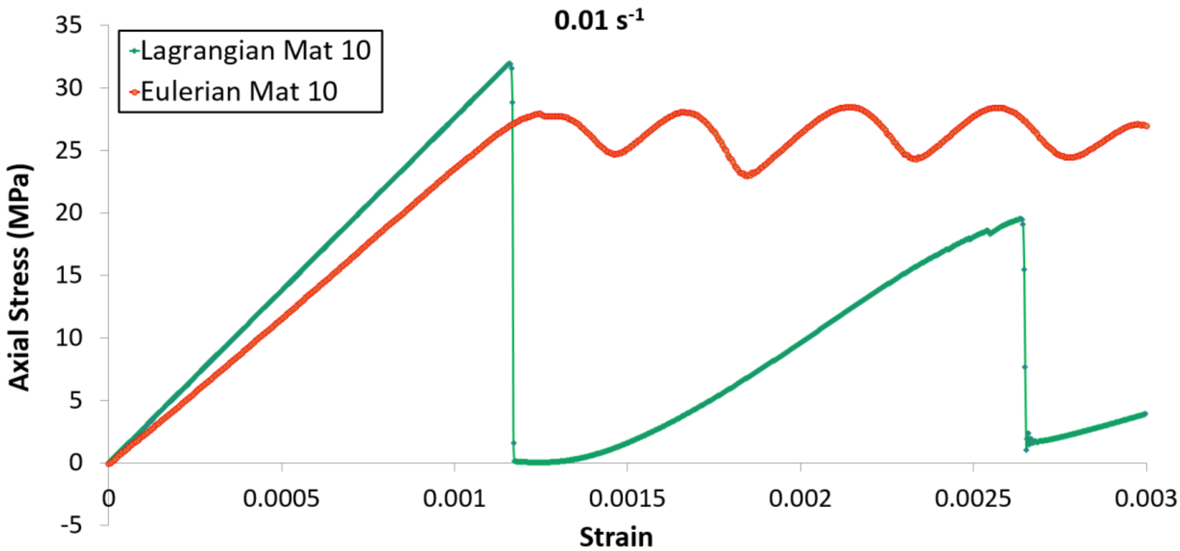

*Fig.7: Axial stress-strain curve at strain rate of 0.01 per second (*MAT_010)*

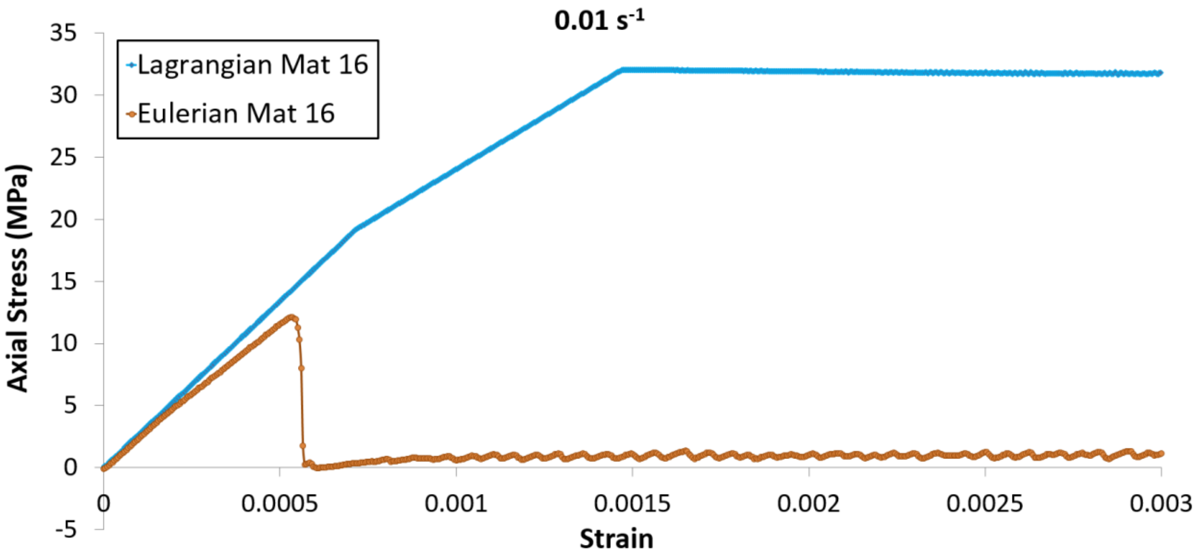

*Fig.8: Axial stress-strain curve at strain rate of 0.01 per second (*MAT_016)*

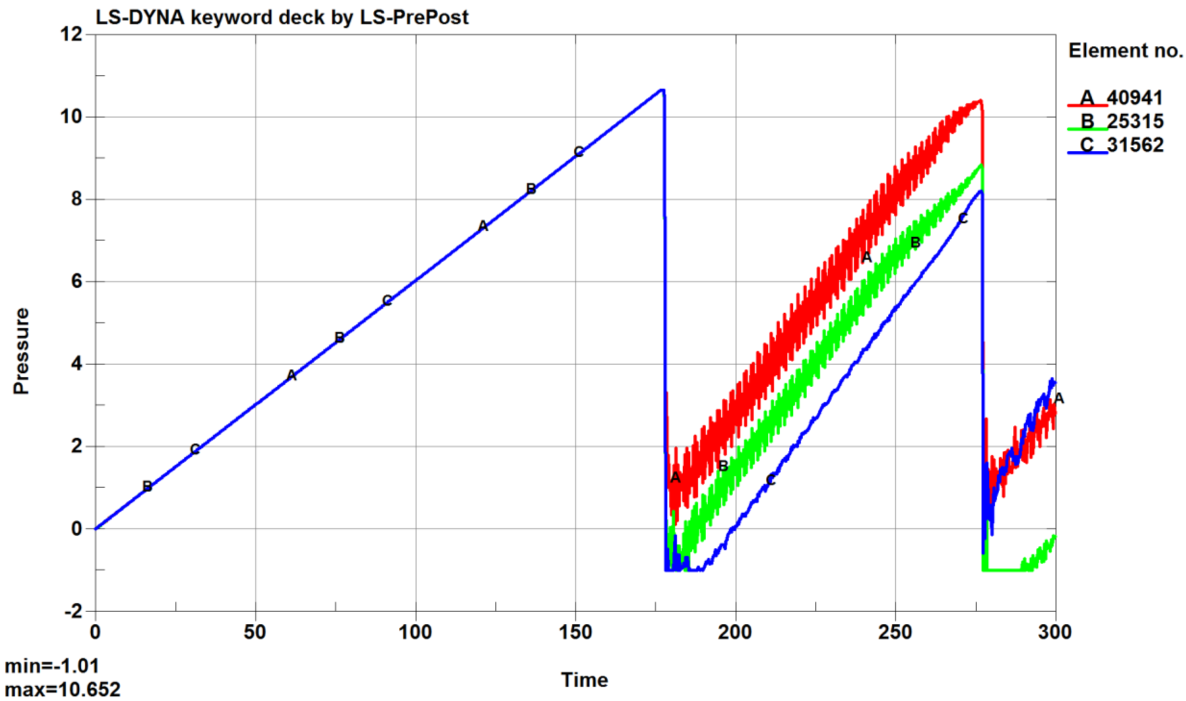

*Fig.9: Mean stress-time curve (*MAT_005)*

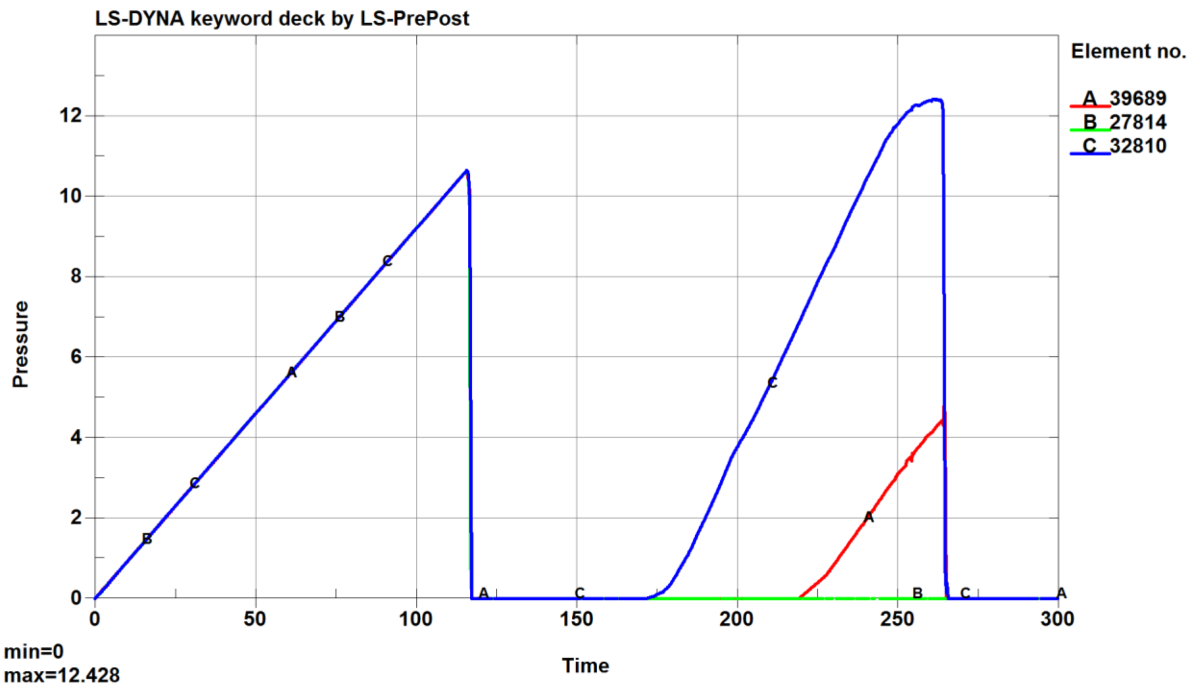

*Fig.10: Mean stress-time curve (*MAT_010)*

<u>Comparison of Concrete Material Models for MM-ALE</u>

From the above observations, of the 3 material models studied, *MAT_005 seemed to be most applicable in modeling the concrete column in this model because the response of the Lagrangian and MM-ALE models did not differ much in response to quasi-static unconfined compression studied in this paper. However, the user needs to take note that this material model does not incorporate damage scaling, or material softening, and will fail suddenly when its pressure cutoff is reached. The implication is that for simulation of cases where concrete is subjected to staged loading (e.g. blast followed by axial compression), the post blast axial capacity of the damaged component may not be so different from the original, as no blast damage will be registered by the material.

*MAT_010 is an alternative to be considered to be used for MM-ALE. The deviation of the response from the MM-ALE models from its Lagrangian counterparts is slightly greater than that for *MAT_005.

MM-ALE model for *MAT_016 exhibited premature failure as compared to its Lagrangian counterpart. As this finding is not well-understood at this point, one has to exercise caution when using *MAT_016 for quasi-static load cases.

4 Blast Loading on Reinforced Concrete Slab – Case Study

Moving on from the above study, *MAT_005 was selected for further investigation by applying it to a blast loading case to assess its suitability for dynamic load scenarios. In this study, a blast[2] test conducted by Engineering Research and Development Center (ERDC) was modeled and the simulation results were compared to the experimental results. The experimental setup of the 1625.6 mm x 958.85 mm x 101.6 mm reinforced concrete slab model was as described in [7]. Figures 11 and 12 show the screenshots of the LS-DYNA model.

[2] A uniform pressure loading on the face of slab is generated by the Blast Loading Simulator (BLS).

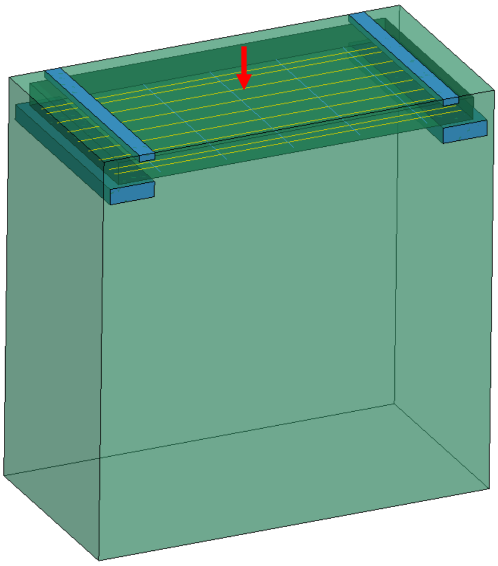

Fig.11: Setup of the blast loaded reinforced concrete slab

Unlike the Lagrangian model where the blast pressure can be applied as segment loading directly on the reinforced concrete slab, it is imperative that the loading condition in the ALE model is properly applied. A pressure-time load curve was applied on the top face of the ALE air domain and allowed to propagate through the air. *BOUNDARY_SPC was applied on the sides of the air domain in the direction perpendicular to its face. Air domain in the direction away from blast was also extended as far as possible such that effect of the blast reflection from the bottom face would be minimized. A tracer was placed just before the reinforced concrete slab to capture the pressure-time history and impulse so as to verify that the correct loading condition was applied (see Figure 13).

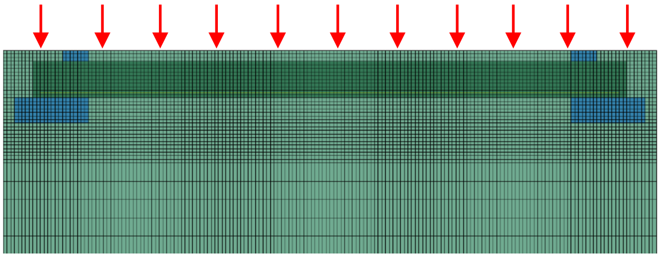

Fig.12: Blast load applied on the top face of the model

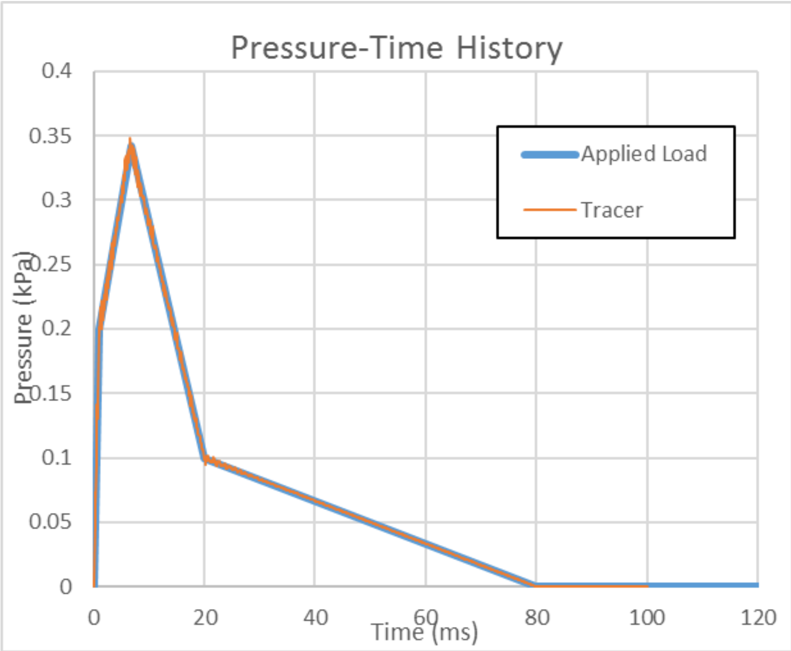

Fig.13: Pressure time history recorded by tracer compared to applied load

```
*SET_PART_LIST_TITLE
Master
$#     sid       da1       da2       da3       da4    solver
        12       0.0       0.0       0.0       0.0MECH
$#    pid1      pid2      pid3      pid4      pid5      pid6      pid7      pid8
         1         3         0         0         0         0         0         0
*SET_PART_LIST_TITLE
Rebar Set
$#     sid       da1       da2       da3       da4    solver
        23       0.0       0.0       0.0       0.0MECH
$#    pid1      pid2      pid3      pid4      pid5      pid6      pid7      pid8
         4         5         0         0         0         0         0         0
*CONSTRAINED_BEAM_IN_SOLID
$#   slave    master     sstyp     mstyp    unused    unused     ncoup      cdir
        23        12         0         0                           2
$#   start       end
```

Fig.14: Coupling of rebar to concrete

A popular method to couple rebar in concrete for Lagrangian simulations is using a constraint-based method. While the same coupling method works for rebar (modeled as beam elements) in ALE concrete, assigning the rebar part (slave) to the concrete part (master) as with typical Lagrangian way of input is a common pitfall among users. As shown in Figure 14, coupling in ALE should make the ALE mesh as “Master parts” which contain both concrete slab (Part 1) and air (Part 3). “Slave parts” in this case refers to the longitudinal (Part 4) and lateral (Part 5) rebar. This allows the coupled nodes (slave) to respond properly when the ALE concrete material moves inside the ALE mesh (master). The available coupling keywords in LS-DYNA are:

- *CONSTRAINED_BEAM_IN_SOLID (CBIS),
- *ALE_COUPLING_NODAL_CONSTRAINT (ACNC), and
- *CONSTRAINED_LAGRANGE_IN_SOLID (CLIS)

These were tested and seemed to be working in the same manner.

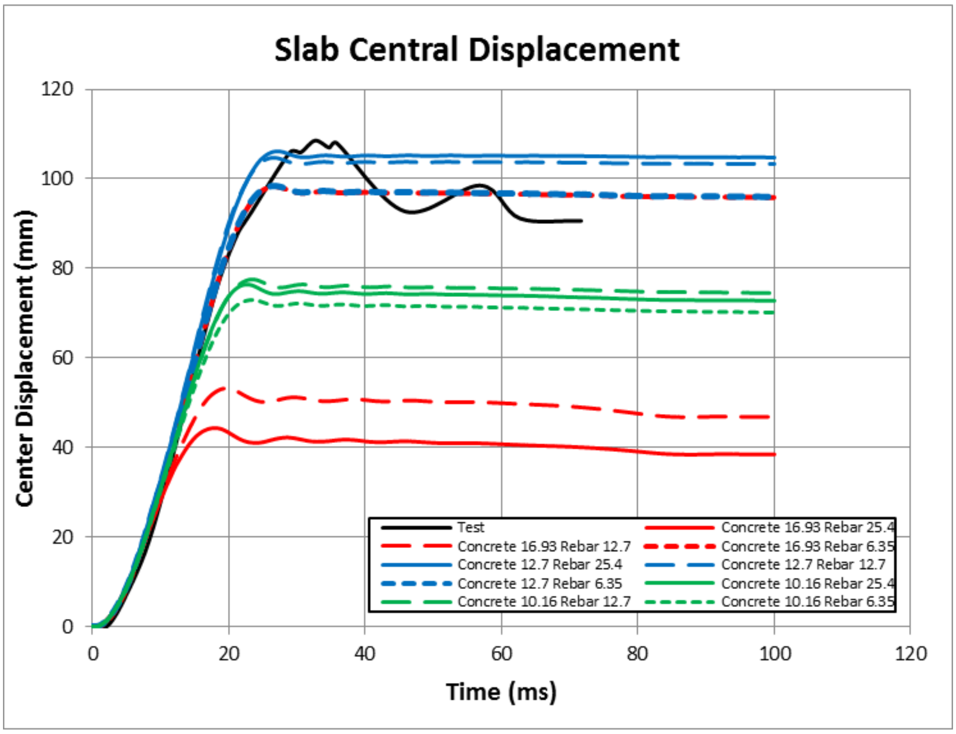

Fig.15: Slab central displacement for ALE reinforced concrete slab

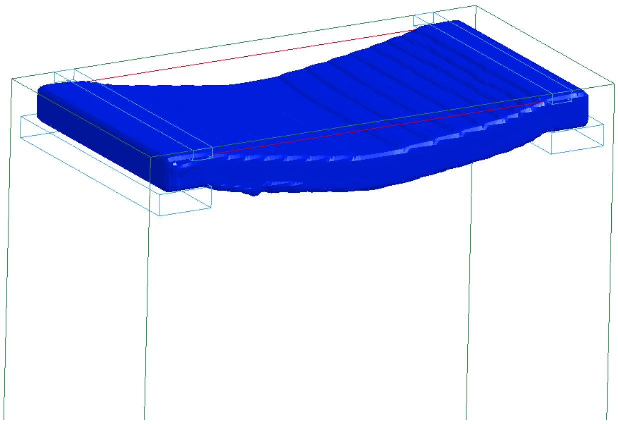

Fig.16: Deflection of the ALE reinforced concrete slab

Figure 15 shows the slab central displacement for the ALE reinforced concrete slab. A total of nine models were tested with varying concrete and reinforcement mesh sizes. Both the meshes of concrete and reinforcement were modeled independently since they can be coupled using coupling keywords. It is observed that the two models using 16.93mm concrete mesh significantly falls short of the experimental deflection measurement although the results improved with finer reinforcement mesh. It is also worth noting that the concrete cover of 12.7mm is in fact smaller than the concrete mesh and may thus have an effect on the results. When the concrete mesh size is held constant at either 12.7mm or 10.16mm, varying the reinforcement mesh size did not result in significant change in the slab displacement. Figure 16 shows the deflection plot of the ALE reinforced concrete slab.

5 Conclusion

When subjected to unconfined compression and air blast at different strain rates, ALE concrete modeled using *MAT_005 provides some meaningful results from the studies made in this paper. While *MAT_005 is a simple concrete model with no damage scaling, strain rate hardening, or softening, it provides a viable alternative for use in MM-ALE to Lagrangian structural response for both quasi-static and dynamic load cases. In addition, like all models, the user has to take into account the mesh sensitivity as demonstrated earlier.

6 References

[1] Swee Hong Tan, Jiing Koon Poon, Roger Chan, David Chng. “Retrofitting of Reinforced Concrete Beam-Column via Steel Jackets against Close-in Detonation”, 12th International LS-DYNA Users Conference, 2012.

[2] Swee Hong Tan, Shih Kwang Tay, Jiing Koon Poon, David Chng. “Fluid-Structure Interaction involving Close-in Detonation Effects on Column using LBE MM-ALE Method”, 9th European LS-DYNA Users Conference, 2013.

[3] Swee Hong Tan, Roger Chan, Jiing Koon Poon, David Chng. “Verification of Concrete Material Models for MM-ALE Simulations”, 13th International LS-DYNA Users Conference, 2014.

[4] Shih Kwang Tay, Jiing Koon Poon, Roger Chan. “Modeling Rebar in Reinforced Concrete for ALE Simulations”, 14th International LS-DYNA Users Conference, 2016.

[5] LS-DYNA R8.0 Keyword User’s Manual II, 2015.

[6] Standard for Verification and Validation in Computational Fluid Dynamics and Heat Transfer, ASME, 2009.

[7] Len Schwer. “Modeling Rebar: The Forgotten Sister in Reinforced Concrete Modeling”, 13th International LS-DYNA Users Conference, 2013.

7 Appendix

1) *MAT_016 Automatic Generated Material Model

*MAT_016 Mode II provides for the automatic internal generation of a simple “generic” model from concrete if A0 is negative then SIGF is assumed to be the unconfined concrete compressive strength, f^1_c and –A0 is assumed to be a conversion factor from LS-DYNA pressure units to psi. (For example, if the model stress units are MPa, A0 should be set to -145.) In this case the parameter values generated internally are:

$$f'_c = \text{SIGF} \qquad a_1 = \frac{1}{3} \qquad a_{0f} = 0$$

$$\sigma_{cut} = 1.7\left(\frac{f'^2_c}{-A0}\right)^{\frac{1}{3}} \qquad a_2 = \frac{1}{3f'_c} \qquad a_{1f} = 0.385$$

$$a_0 = \frac{f'_c}{4}$$

Note that these a_{0f} and a_{1f} defaults will be overridden by non-zero entries on Card 3. If plastic strain or damage scaling is desired, Cards 4 through 7 and *b*1 should be specified in the input. When a_0 is input as a negative quantity, the equation-of-state can be given as 0 and a trilinear EOS Type 8 model will be automatically generated from the unconfined compressive strength and Poisson’s ratio. The EOS 8 model is a simple pressure versus volumetric strain model with no internal energy terms, and should give reasonable results for pressures up to 5kbar (approximately 75,000 psi).

2) Calibrating *MAT_005 and *MAT_010

Several of the LS-DYNA concrete constitutive models are capable of generating all their necessary input parameters using internal algorithms based on specifying the unconfined compressive strength of the concrete. Any of these ‘simple’ models may be used to generate material characterization data that can be best fitted by those material models that do not provide for parameter generation, e.g. *MAT_005 and *MAT_010.

As an example, *MAT_72R3 is one of the ‘simple input’ concrete models that when supplied with an unconfined compression strength and Poisson’s ratio will generate a three parameter shear failure surface and a pressure versus volume strain relation. The three parameter shear failure surface can then be used to generate data suitable for a best fit by other constitutive models; similarly, the pressure versus volume strain relation can be best fit. The two *MAT_72R3 elastic constants, i.e. input Poisson’s ratio, and elastic bulk modulus obtained from the initial slope of the pressure versus volume strain relation, can be used with Hooke’s law to provide any other necessary elastic constants.